Development of an Unsteady BET Model for Forward Flapping Flight: Performance Comparison of Different MAV Configurations

Pedro Scotti Campos Belo Afonso
pedro.scotti.afonso@tecnico.ulisboa.pt

Instituto Superior Técnico, Universidade de Lisboa, Portugal

October 2018

Abstract

This work set out to develop an aerodynamic model describing flapping wing forward flight, starting from two existing models for hovering flapping flight and resorting to the Blade Element Theory, as well as unsteady aerodynamics concepts. The developed model was later fitted into an user-friendly tool that allows for the optimization process of a flapping wing to be dramatically sped up, and served as the basis for a performance comparison between the flapping wing and the more traditional flight solutions like the fixed and the rotary wing. The comparison was also done in a purely analytical way, through the manipulation of power equations, so as to provide various methods to compare the different configurations. The analytical results show that, in some situations, the flapping wing has the edge in terms of power consumption. However, the results obtained by the tool show that in every case studied here the other configurations consume less power. Nevertheless, since the flapping wings that were put to the test were only optimized in a rudimentary way, and given that several cases remained unstudied, we cannot affirm that there are no situations where the flapping wing is advantageous. It can only be said that, in very specific cases, this configuration showed to perform worse than its counterparts.
Keywords: Flapping Wing, Comparison, Blade Element Theory, Power, Unsteady Aerodynamics

1. Introduction

Engineers have spent the better part of the last century trying to improve the flight solutions already proven to work, namely fixed-wings and, to a smaller extent, rotary wings. However, these solutions can only improve so much, and the search for the next big breakthrough in the aerospace field is on. Through countless years of evolution, Nature has reached the state of near perfection when it comes to flying animals. Birds and insects are capable of extraordinary feats such as long-range flight, high-thrust propulsion and efficient hovering, some of which going as far as to combine several of these capabilities. All of this is due to wings that evolved to be as efficient and lightweight as possible, while remaining manoeuvrable enough to give flyers a wide range of movements. In short, there is a lot of knowledge that can be taken from Nature, but so far this objective has proven elusive for engineers due to the difficulty in studying the aerodynamic and mechanical behaviour of these animals. Computational models describing flapping flight already exist, but they are either too costly or too specific; a simpler, more flexible and more affordable model that maintains the accuracy of the more sophisticated methods could then help in the quest to understand flapping flight. There is undoubtedly a need for more efficient aircraft, and now is the time to analyse the pros and cons of flapping flight and, if proven to work in a real-life implementation, to push for its widespread adoption. However, the tools for such a detailed study are not yet readily available, and this work sets out to develop a model that quickly predicts both aerodynamic loads and power consumption of a flapping wing vehicle. Birds have cracked the code of efficient flight, so why can't we?

1.1. State of the Art

The subject of performance comparison between different propulsion strategies has seen several developments during the recent past. The work by Liu and Moschetta [6] tried to compare the hovering power expenditure of two different Micro Air Vehicle (MAV) configurations, rotary and flapping wings, having reached the conclusion that, based on a theoretical approach, there is not an appreciable difference between the designs. Pesavento and Wang [9] set out to find if there was a flap-

ping wing configuration that could prove to be more efficient than its fixed wing counterpart. Through the use of CFD and optimization of the flapping wing, they showed that it was possible to get a configuration that consumed 27% less power than an identical fixed wing. The topic of rotary vs. flapping wings was again explored by Zheng et al. [14], using CFD, and the conclusion was that for small Reynolds numbers ($Re < 100$), flapping wings have a lift-to-power ratio twice as large as the rotating configuration. More recently, flapping wings were again compared to fixed wings by Sachs [11] from a mathematical standpoint. The conclusion was that, for low induced drag factors, flapping wing vehicles show a higher efficiency, therefore requiring fixed wing vehicles to have a higher propeller efficiency in order to yield a comparable flight performance.

Regarding the topic of flapping flight models, even though forward flight remains very much unexplored due to the difficulty of the analysis and to the wide range of factors that play a role in this type of movement, some attempts have been made to describe the hovering state. Perhaps the most famous one, Dickinson et al. [3], tried to predict the forces generated by a *Drosophila melanogaster* (fruit fly). The values were then compared to those of a mechanical wing, and the generated forces were attributed to three different mechanisms: delayed stall, rotational circulation and wake capture. As a response to this work, Walker [13] created a very detailed Unsteady Blade Element Theory (UBET) model of the forces that arise from a hovering wing and paved the way for what would later become one of the modified models of the present work. In his study, he found evidence supporting the thesis that rotational forces are indissociable from the translational component of the forces, and could explain Dickinson's measurements using this idea. After comparing the results to both a quasi-steady model and CFD measurements of the same wing, the conclusion was that the UBET model was a viable option to predict how freely flying animals move. Another study aimed at creating an UBET based model was the one by Truong et al. [12], that set out to recreate the values measured by Dickinson et al. [3] through the modification of a normal Blade Element Theory (BET) model. After dividing the forces into different components, namely translational, rotational and apparent mass, the work describes the model's implementation, validation and subsequent application to the case of a beetle. The authors showed that the model was able to achieve values very similar to those measured in the original article, suggesting that their model was accurate enough to be used as a standalone method in different cases. Due to the potential showed by both this method and Walker's, these were chosen as a the building blocks of the analysis later done in this report.

As previously stated, even though all of the mentioned studies apply to the case of hovering vehicles, the same search focused on a BET model for forward flapping flight yields no results. Nonetheless, the existence of so many hovering models suggests that an UBET model could be modified to accommodate for the differences that forward flight presents. This model could then be validated by values obtained through a more sophisticated CFD analysis, like the one by Choi et al. [1], where the objective was to find the most effective flapping motions and how that influenced the overall performance of the vehicle. In doing so, this work provided valuable force measurements that were used for the validation of all the UBET models developed in this work.

2. Background

2.1. Power Consumption

For the first part of the work, the power equations of the three different configurations have to be established. For the fixed wing Sachs' approach [11] was used, resulting in the power expression

$$P_{fix} = \frac{\rho}{2\eta_{prop}} A_w V_\infty^3 \left(C_{D0} + \frac{C_L^2}{\pi \text{Æ} e} \right), \quad (1)$$

where ρ is the fluid density, η_{prop} is the propeller's efficiency, A_w is the area of the wing, V_∞ is the free stream velocity, C_{D0} is the profile drag coefficient of the wing, C_L is the lift coefficient, Æ is the aspect ratio of the wing and e is Oswald's efficiency factor. As for the rotary wing, Leishman's procedure [5] was used, that defines the power consumed as

$$P_h = \rho A_h V_{tip}^3 \left[\frac{\sigma C_{D0}}{8} \left(1 + K\mu^2\right) + \frac{\kappa C_T^2}{2\sqrt{\mu^2 + \lambda^2}} \right], \quad (2)$$

where A_h is the rotor disc area, V_{tip} is the speed of the blade tip, σ is the rotor's solidity, K is an empirical correction factor for profile power, μ is the advance ratio, κ is an empirical correction factor for induced power, C_T is the thrust coefficient and λ is the inflow ratio. Finally, again according to Sachs [11], flapping wing power consumption is given by

$$P_{flap} = \frac{1}{2} \rho A_w V_\infty^3 \gamma_{av}^{-3/2} \left(C_{D0} + \frac{C_{L,vert}^2}{\pi \text{Æ} e_{flap}} \right), \quad (3)$$

where γ_{av} is the average flapping angle, $C_{L,vert}$ refers to the vertical component of the lift coefficient and e_{flap} is the modified Oswald coefficient to account for the flapping wing effects.

2.2. Forward Flight BET

The issue of describing forward flight through a BET model has been tackled by Leishman [5] be-

fore. Since the original case was applied to helicopters, here there is a selection of only the parts that concern flapping flight, not rotary wing flight. The scheme used was that of Figure 1. The pro-

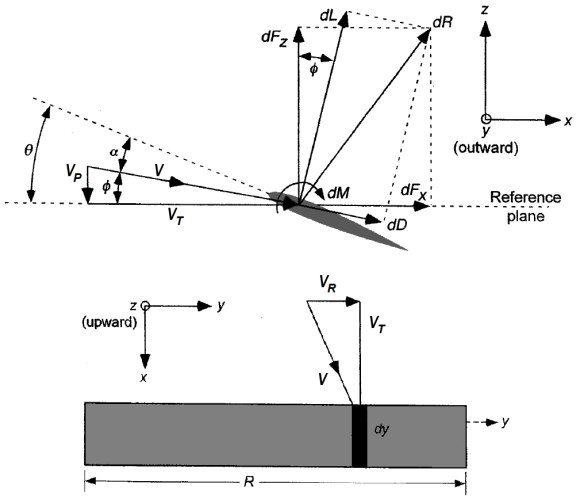

Figure 1: Top and side view, respectively, of the reference scheme and wing environment used throughout this work (adapted from [5])

cedure to determine blade forces begins by finding the different velocities at each element, which are divided into three categories: translational (V_T), vertical (V_P) and radial (V_R). Knowing the velocities, it is possible to calculate the induced angle of attack ϕ, depicted in Figure 1, defined as $\phi = \arctan(V_P/V_T)$, which in turn renders out the aerodynamic angle of attack (AoA) as $\alpha = \theta - \phi$, where θ is the pitch angle of the airfoil. This value is then used to evaluate both the lift and drag coefficients, and having these values one can calculate the incremental lift and drag in each section

$$dL = 0.5\,\rho\,V_\infty^2\,c\,C_l\,dy\,, \tag{4}$$

$$dD = 0.5\,\rho\,V_\infty^2\,c\,C_d\,dy\,, \tag{5}$$

where c is the chord length. Using Figure 1 as a reference, solving for the vertical and horizontal forces acting on the blade renders out

$$dF_z = dL\cos(\phi) - dD\sin(\phi)\,, \tag{6}$$

$$dF_x = dL\sin(\phi) + dD\cos(\phi)\,. \tag{7}$$

Finally, to obtain the total values along the wing and during an entire rotation, one must integrate these values along the blade's length.

2.3. Truong's Hovering Flapping Wing Model

Based on the 1999 findings by Dickinson et al. [3] regarding force generation by an insect wing in a hovering state, Truong and his team developed a paper detailing an UBET based model that could approximate the average forces measured by Dickinson with an estimated error of only 5.7% [12].

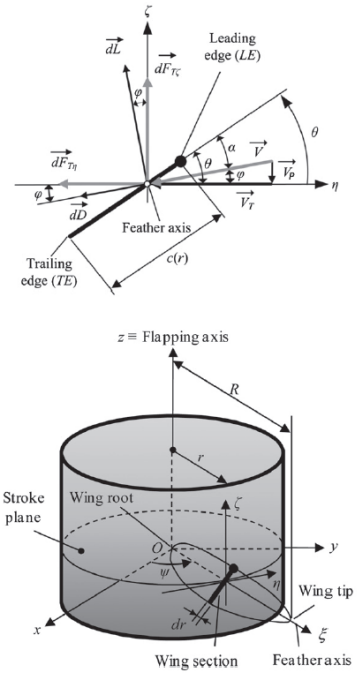

Figure 2: Scheme and variables used by Truong for the development of the model [12].

Their method is based on a normal BET analysis, the difference, however, is that generated forces are divided into three components (translational, rotational and added mass). The translational component is the force that would be generated by a static airfoil flying at the same speed. It is defined as

$$F_{T,\zeta} = \frac{\rho}{2}\int_0^R c\,(C_l\,V_T - C_d\,V_P)\,V\,dr\,, \tag{8}$$

$$F_{T,\eta} = \frac{\rho}{2}\int_0^R c\,(C_l\,V_P + C_d\,V_T)\,V\,dr\,. \tag{9}$$

Truong defines $V_T = \dot{\psi}r$ and assumes a $V_P = 0$, resulting in a null induced AoA, while V is the total speed. While these assumptions do not affect the calculations for the hovering case, further down the road the implications of this simplification will become apparent. Rotational force, another component of the total force, is the one that comes from the circulation around the wing. It is given by the expression

$$dF_{rot} = \rho V_T\,d\Gamma_{rot}\,, \tag{10}$$

where $d\Gamma_{rot} = G\dot{\theta}c^2\,dr$, with G being the rotational force coefficient. G is calculated in one of two ways: for every element the value of $\omega = \dot{\theta}c_{av}/V_T$ is calculated, and if the value is between 0.166 and 0.374, G is obtained through the work by Dickinson and Sane [2]. If the value does not fit into these limits, the relation $G = \pi(0.75 - x_f)$ is used, where x_f is the dimensionless distance from the leading edge to the rotation axis. This is the truly unsteady part of the model, since for different values of ω, various values of G will arise. Finally, the added mass force

is defined as the component that appears as a reaction to the wing pushing the air around it during its movement, given by the expression

$$dF_A = \frac{\pi}{4}\rho c^2 a_\perp \, dr \,, \tag{11}$$

where $a_\perp$ is the component of the acceleration normal to the wing. To obtain the instantaneous total values one must simply integrate the values along the wingspan and project the forces into the inertial reference frame. Looking at the results, shown in Figure 3, it is clear that the model can describe the overall aerodynamic behaviour of the wing accurately. The model does show some limitations, however, as one can tell looking at the peaks in force generation. Even though the curves follow the overall trend of force generation, they do not reach the maximum measured drag and lift forces, and both drag peaks are shifted to the right. It is, nonetheless, a very good approximation since this is a model that can run almost instantly, compared to the several hours the same CFD analysis would take.

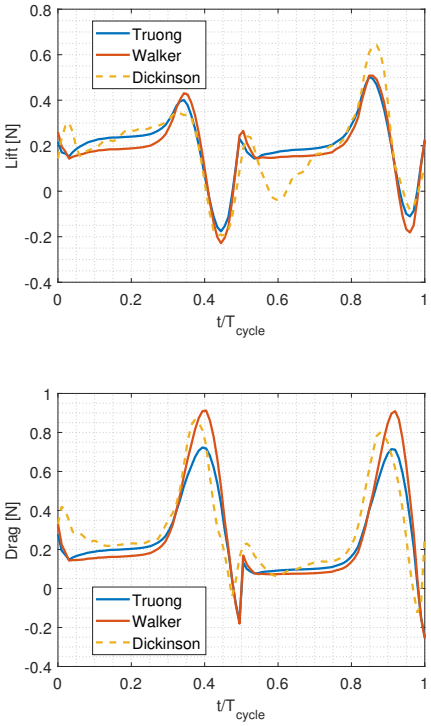

Figure 3: Results yielded by the Truong and Walker models, and comparison with the measurements obtained by Dickinson et al. [3].

2.4. Walker's Hovering Flapping Wing Model

In his 2002 paper [13], Walker focuses on the importance of rotational lift for hovering flapping flight. His main objective was to find just how essential rotational lift is for the hovering aerodynamics of insects and birds, and if there was any truth to the thesis put forward by Dickinson that the force peaks were caused by the interaction between the wing and its previously shed wake. To test his hypothesis, he developed an aerodynamic model of the flapping wing, following the scheme showed in Figure 4.

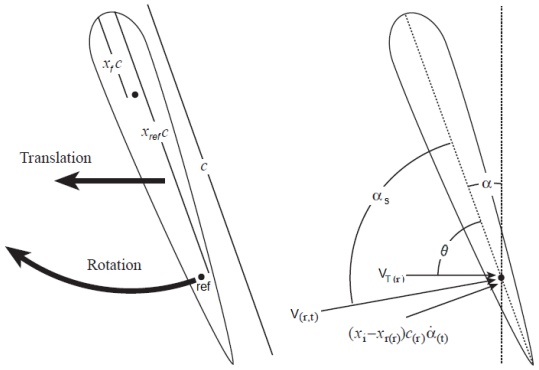

Figure 4: Scheme and variables used by Walker for the development of his model (adapted from [13]).

The big difference from this model to the previous one is the definition of the velocity components and the angles. Whereas Truong assumed a null V_P, Walker defines the velocities in terms of parallel and perpendicular to the wing, never ignoring any speed term, through the expressions

$$V_\perp = V_T \cos(\alpha) + (x_{ref} - x_f)\, c\, \dot{\alpha} \,, \tag{12}$$
$$V_\parallel = V_T \sin(\alpha) \,, \tag{13}$$

and then defines the angle of incidence as being $\alpha_s = \arctan\left({}^{V_\perp}/_{V_\parallel}\right)$. He also uses a reference point which is not coincident with the rotation axis, so the rotational velocity is also accounted for in the calculations. As for the forces, Walker chooses to group together into a component called circulatory-and-attached-vortex the forces that Truong defined as the translational and rotational components, so in this aspect the difference between models is only in terms of semantics. This component is first calculated relative to the local stream through

$$dL_s = 0.5\, V^2 c\, \Phi C_l \, dr \,, \tag{14}$$
$$dD_s = 0.5\, V^2 c\, \Phi C_d \, dr \,, \tag{15}$$

where Φ is the Wagner function, or the term that accounts for the unsteady effects of instantaneously rotating and flapping the wing, and V is the total speed. These dL_s and dD_s components are then projected into the inertial reference frame, which corresponds to a projection about θ. The other component of the force is the added mass force, which in no way differs from Truong's definition. To obtain the total values, one must again integrate the infinitesimal forces along the wingspan and during the flapping cycle.

3. Preliminary Power Consumption Analysis

The first part of the implementation in this work was based on the premise of finding an analytical way to compare the three flying configurations. The comparison was achieved by manipulating Equations 1, 2 and 3 in three different cases, fixed vs. rotary, fixed vs. flapping and finally rotary vs. flapping. The manipulation consisted in dividing the respective power equations of each case, equalling the result to 1 and then isolating one variable. After this typical values were assumed for all other variables except speed, which resulted in a curve representing the critical value that the isolated variable must take for the power consumptions to be identical, effectively dividing the areas where each configuration consumes less power.

3.1. Fixed vs. Rotary Wings

For this analysis the isolated variable was η_{prop}, the propeller's efficiency, following Sachs' example [11]. Looking at the results of Figure 5, which were obtained using the standard values of $\mathit{AR} = 3$, $\kappa = 1.75$, $\alpha = 2°$, $N_b = 2$, $\mathit{AR}_b = 4$, $C_{D0} = 0.035$, $K = 4.6$, $e = 0.8$, it becomes clear that the fixed wing has the edge, as for the given speed interval (defined in terms of the rotary wing's advance ratio), the fixed wing would need to have η_{prop} values of around 40% for its power consumption to be worse than that of a similar rotary wing, a smaller value than what we normally observe.

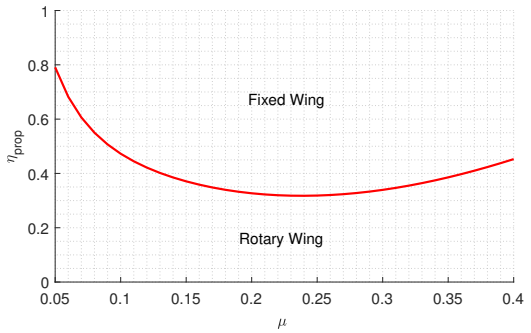

Figure 5: Curve that divides the areas where the fixed wing is preferable (above the curve) from the area where the rotary wing is more efficient (below the line).

Performing a parametric study, the following conclusions are drawn: increasing the aspect ratio of the fixed wing increases the area where the fixed wing is preferable, and assuming the same C_{D0} for both wings, we see that the lower it is the more the rotary wing benefits. The number of blades of the rotary wing has differing results depending on the speed (more blades are beneficial for the rotary wing at lower speeds, detrimental at higher speeds), and finally the aspect ratio of the rotary wing also showed differing results, but, in general, the rotary wing benefits from having blades with a higher aspect ratio.

3.2. Fixed vs. Flapping Wings

In this case the isolated variable was also the propeller's efficiency, but this time the results are plotted as a function of forward speed, not advance ratio, because of the similarities between the configurations. The curve was plotted assuming $\rho = 1.224\,\mathrm{kg/m^3}$, $m = 50\,\mathrm{g}$, $\mathit{AR} = 3$, $b = 20\,\mathrm{cm}$, $C_{D0} = 0.035$, $e = 0.8$, $\gamma_{max} = 60°$ and dimensionless lift fluctuation factor $\Delta = 1$, and it is shown in Figure 6.

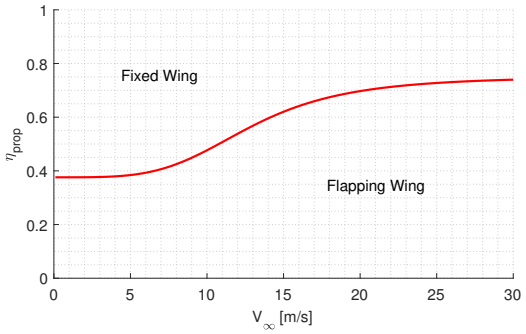

Figure 6: Curve that divides the areas where the fixed wing is preferable (above the curve) from the area where the flapping wing is more efficient (below the line).

The results show how, for small speeds, the fixed wing is preferable, as only having a propeller efficiency smaller than $\eta_{prop} = 40\%$ would render it a worse option than the flapping wing. For higher speeds, however, the flapping wing becomes a more viable option. As for the parametric study, increasing the flapping angle γ_{max} showed to worsen the performance of the flapping wing, while decreasing the aspect ratio of both configurations seems to benefit the flapping wing. Bigger and heavier configurations show to favour the fixed wing, and finally, the most influential parameter was Δ, the dimensionless lift variation, which quantifies the fluctuations in the lift vector during the flapping stroke. The bigger this factor, the worse the overall performance of the flapping wing is.

3.3. Rotary vs. Flapping Wings

Here the isolated variable was Δ, for being the hardest parameter to quantify. The curve was drawn using all of the standard values specified in both in subsection 3.2 and subsection 3.1, and it is shown in Figure 7. The rotary wing shows to be preferable in a large portion of the graph, namely above $\mu = 0.32$ ($V_\infty = 18\,\mathrm{m/s}$). For lower speeds, the flapping wing normally has the edge, since only high fluctuations of the lift ($\Delta > 1$) render it less efficient than the rotary wing. Regarding the parametric study, the aspect ratio of the flapping wing shows to be crucial to its power consumption, as any increase in this value means very significant gains performance-wise. The same happens with the blade's aspect ratio, the higher it is the better

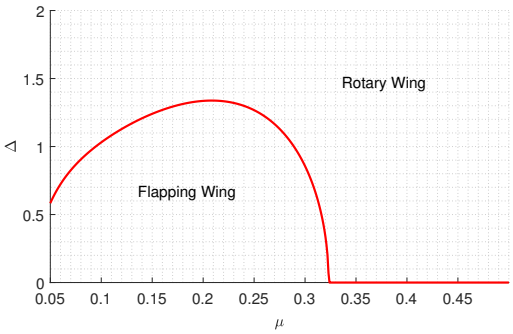

Figure 7: Plot of the curve that divides the areas where the rotary wing is preferable (above the curve) from the area where the flapping wing is more efficient (below the line).

the rotary wing's performance. Increasing the flapping angle also results very prejudicial to the flapping wing, and adding more blades to the rotary wing worsens its performance.

4. Development of an UBET Model for Flapping Wing Forward Flight

The process of developing an UBET specifically for flapping wings starts by implementing the models for hovering flapping flight developed by Truong and Walker, discussed in subsection 2.3 and subsection 2.4, and then modifying them to accommodate for the changes that forward flight demands. Finally, a combination of the two models is created, since this proved to achieve better results than each of the individual modified models.

4.1. Truong's model implementation & adaptation

The original hovering model was implemented using MATLAB and follows the following logic: it starts by defining the number of elements for the analysis, both in terms of span and time. Then it calculates the chord for every point, according to the procedure by Ellington [4], which serves the objective of mimicking Dickinson's conditions [3] to then validate the model with his measurements. Using the values also defined by Dickinson for angular and translational velocity, it calculates the speeds and accelerations for every point of the wing. Then the angles for the downstroke are transformed through $\theta = \pi - \theta$, since the movement is reversed, and with these new values the C_l and C_d of each element are evaluated. Now the infinitesimal forces in each element can be calculated, and the routine ends with the integration along the wingspan and subsequent plotting of the results, which are displayed in Figure 8.

The modification for the forward flight case is based on two premises: the inclusion of a vertical velocity component (see Figure 2) and a rotation of the inertial axis, purely for convenience reasons. This mainly impacts the calculation of the velocities in each element, which are now $V_\zeta = V_\infty$ and $V_\eta = \dot{\psi}\, r$. Even though Truong ignored the effects of an induced angle of attack in the hovering model, this is not an option now as the free stream and flapping speeds are of the same magnitude, which would lead to wildly inaccurate values. So the induced AoA is calculated through $\phi = \arctan\left(V_\eta / V_\zeta\right)$, and is later subtracted to the geometric angle of attack θ to uncover the effective AoA, which is used in the lift and drag coefficient evaluation. For the C_l and C_d values, since the angles go almost up to 80°, it was decided to use the work by Leishman [5, p. 409] on the static lift and drag coefficients of a NACA 0012 airfoil at extreme angles of attack and low Mach values, which is also the approach used by Pourtakdoust and Aliabadi [10]. The validation of the model was done resorting to the work by Choi et al. [1], which studies the optimum rotational and flapping movement of a 2D airfoil through a CFD analysis. It concludes that, for a flapping frequency $f_{flap} = 9.55\,\text{Hz}$, $V_\infty = 3\,\text{m/s}$, $Re = 10^4$ and reduced frequency $k = 1$, the optimum movement of the wing is given by $\theta(t) = 30\cos(\omega t + 97.6624)$ and $\gamma(t) = 53\cos(\omega t)$. Isolating one element of the model and introducing these parameters into the simulation results in the curve shown in Figure 8.

As it can be seen, even though the values do follow the overall trend of the the curve obtained by Choi, there are some problems with the model. Regarding lift, not only does the model underestimate the peak value by more than 100% of its value, an unacceptable result by all measures, but there is a noticeable offset between the curves. Drag also shows values that do not seem fitted to the reference curve, with a big underestimation of the peaks (almost by 50%) and a clear offset of the curve to the right. This offset suggests that the model might have a problem with the definition of its aerodynamic angles, causing its continuous delay in force prediction.

4.2. Walker's model implementation & adaptation

The implementation of this hovering model was very similar to the previous one. The first difference appears when defining the velocities and the effective angle of attack, as Walker divides the speed into two categories, parallel and normal to the wing (see Equations 13 and 12), and with these values calculates the angle of incidence. So the definition of the angle of attack is the main difference in implementation between the two models, as Truong's model doesn't admit the scenario of velocity-induced changes to the angle of attack, while Walker's does. The other difference is related to the definition of the forces, which, as discussed in subsection 2.4, are not the same as for the previous model. The hovering model was implemented here, yielding the results shown in Figure 3. As for the

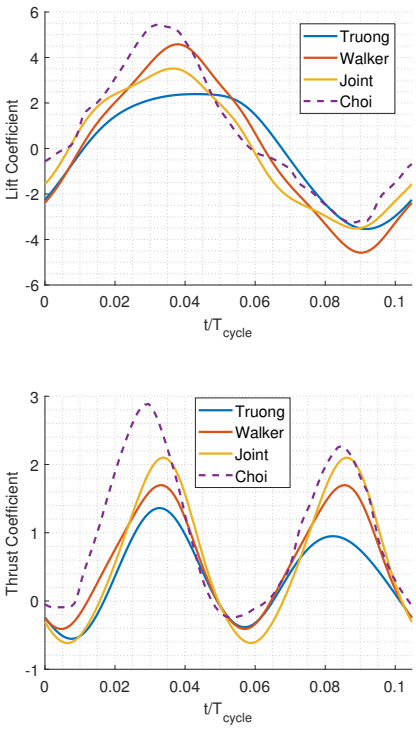

Figure 8: Results yielded by Truong and Walker modified models, as well as the joint model, compared to the results obtained by Choi et al. [1].

adaptation to the forward flight case, the logic is the same as before. The velocities here become

$$V_{\perp} = V_T \cos(\alpha) + (x_{ref} - x_f)\, c\, \dot{\alpha} - V_{\infty} \sin(\alpha)\,, \tag{16}$$

$$V_{\parallel} = V_T \sin(\alpha) + V_{\infty} \cos(\alpha)\,. \tag{17}$$

which is a better approach than Truong's since it accounts for the rotation of the wing, producing a more accurate induced angle of attack, which can clearly be observed in Figure 8, which is the validation of this model against Choi's work [1]. Analysing the image it becomes clear that the problems, albeit slightly diminished, have not disappeared. The curves follow the general trend of the reference values and the problem of the underestimation of the thrust peaks is now a little less pronounced, but at the same time it has room for improvement, as it will become apparent after the development of the joint model.

4.3. Joint Model

The two previous models have some clear problems, namely the curve offsetting and peak force underestimation, making it clear that some adjustments have to be made. It only seems reasonable that, in order to build a more advanced UBET model for flapping wing forward flight, the best approach will consist of isolating the best aspects of each of the previous models, combine them into just one and try to adjust the equations to better describe the physical reality of a flapping wing MAV.

The joint model includes the forces definition by Truong et al. [12] (added mass, circulatory and translational) that proved to describe the reality in a consistent way, while also making use of the velocities and angles as they were defined by Walker [13]. The implementation of this new model is in every way similar to the others before it, so a detailed explanation will not be presented here. Instead, a brief overview will be given, touching all the relevant subjects. Using Truong's model as the base, since in its core the new model will resemble it more than Walker's, the velocities were changed to follow Walker's approach. This has the immediate effect of changing the angle calculation, which was arguably the weakest point in this model. The new speeds also impact the rotational force calculation, since the velocity is an integral part of its equations, and affect the translational force in several ways, given that this component (which is the biggest contributor to the total force) depends directly on the speeds, angles and finally on the drag and lift coefficients (which are calculated directly through the induced angle of attack, again emphasizing the importance of the angle calculation). This approach produces the results shown in Figure 8, confirming that joining the models and applying the described changes culminates in better results than those of the previous separated models. It is also the reason why, when building the companion tool to this work, this was the chosen model.

5. Refined Power Consumption Analysis

5.1. Parametric Study

The final part of this work consists in, through the use of the joint model-based tool developed for the project, analysing the effects of each design parameter of the flapping wing on its performance, to execute a simple optimization of a given wing and compare its power consumption to that of a fixed and a rotary wing of similar specifications.

The first parameter to be studied is mass, and the interesting aspect to this parameter is to watch how the optimum V_{∞} and f_{flap} vary with the increasing mass, according to Pennycuick's relations [8], which were adapted to the specific case of MAVs

$$f_{flap} = 2.16 m^{1/3} g^{1/2} b^{-1} A^{-1/4} \rho^{-1/3}\,, \tag{18}$$

$$V_{\infty} = 5.12 (mg)^{1/2} b^{-1} \rho^{-1/2}\,. \tag{19}$$

Aside from this, the obvious conclusion is that the lighter the aircraft, the better the performance. As for the aspect ratio, we observe than an increase in this parameter results in lower forces and power consumption. The only downside to this decrease is in terms of thrust, meaning that the steady-state forward speed, or the speed of null net forces applied on the vehicle, will be significantly smaller.

The maximum flapping angle analysis shows that there is a minimum value that generates just enough lift for the aircraft to remain airborne, and that increasing this value any further is very penalizing in terms of power consumption, so the design point should be defined as this one.

On the other hand, the maximum rotation angle θ_{max} deeply influences the lift and thrust production. Increasing this angle makes both the thrust and lift grow at first, but at around $\theta_{max} = 30^\circ$ for thrust and $\theta_{max} = 40^\circ$ for lift they hit a peak, decreasing quickly afterwards. Power consumption decreases steadily throughout the analysis, suggesting that the bigger this angle, the better, but a balance must be struck with the force generation, so a value around 35° should be adequate for most cases. The average pitch angle, θ_{av}, is the angle around which the sinusoidal pitching movement is performed. Varying this value we see that its greatest impact is in terms of the lift, which is very sensitive to this angle, increasing substantially with any increment to θ_{av}. The power consumption remains undisturbed for small values of θ_{av}, and suddenly increases significantly for angles bigger than 5°, suggesting that the best compromise can be to find the $\theta_{av,crit}$ for sufficient lift generation and use it as the design point.

Contrarily, the dimensionless rotation center, x_f, seems to only affect the thrust, with a very small variation in power consumption. This makes it a very useful parameter to easily adjust the speed of the vehicle without compromising other aspects of the design. Wingspan, when incremented, showed to increase both the forces and power consumption. This suggests that the lowest possible value of b that generates enough lift should be chosen as the design point. Flapping frequency was probably the variable that most affected the overall performance; an exponential increase in power consumption could be observed as the frequency started to climb, accompanied by a increase in lift and thrust generation, though smaller in magnitude. This again indicates that the minimum value of f_{flap} must be found to maximize the efficiency of the vehicle.

5.2. Flapping vs. Fixed Wing

Resorting to the conclusions drawn from the parametric study, followed by a *Steady State Analysis* (a functionality of the tool dedicated to finding the point where zero net forces are applied on the vehicle), it is possible to design a flapping wing that, through an optimization process, can be put to the test against similar rotary and fixed wings. For the fixed wing, the comparison term was selected to be the flying wing studied by Ostler et al. [7], characterized by $m = 0.95\,\text{kg}$, $b = 1.06\,\text{m}$ and $\mathit{AR} = 3.5$. Three cases were put to the test, to observe the benefits of the optimization. In the first case the flapping wing has three shared parameters with the fixed wing: mass, wingspan and aspect ratio. In the second case only the mass and the wingspan are identical, and for the last case the only restriction is $m = 0.95\,\text{kg}$. This procedure yields the results shown in Table 1.

Parameter	Case 1	Case 2	Case 3
m [kg]	**0.95**	**0.95**	**0.95**
b [m]	**1.06**	**1.06**	0.92
AR	**3.5**	2.7	2.2
f_{flap} [Hz]	5.22	4.28	4.78
V_∞ [m/s]	14.2	13.9	14.4
x_f	0.22	0.27	0.24
γ_{max} [°]	38	39	39
θ_{max} [°]	42	40	39
θ_{av} [°]	15	15	18
Lift [N]	9.381	9.362	9.428
Thrust [N]	0.085	0.093	0.209
Power [N]	82.21	72.37	71.40

Table 1: Parameters and configuration performance metrics resulting from the optimization process.

These same results were plotted in Figure 9 alongside the power curve of the flying wing. What can be observed is that, through this rudimentary optimization, values of power consumption which are similar in magnitude to those of the fixed wing were obtained. Not only that, it can be seen how more freedom in terms of parameter variation, meaning more flexibility design-wise, allowed for the discovery of increasingly better solutions to save power. The results in terms of general optimization were not, however, as pronounced as desired, further reinforcing that a more sophisticated optimization process is required to achieve better results. It is not unreasonable to assume that there might be a combination of parameters that allows the flapping wing to outperform the fixed wing, but, as far as can be extracted from this test, the performances are really quite distinct, since the best flapping still consumes twice as much power than the equivalent fixed wing. So, in short, what can be drawn from this study is that for approximately the same specifications, the fixed wing has the edge in terms of power consumption.

5.3. Flapping vs. Rotary Wing

The case of rotary wings is somewhat more complicated due to the lack of information on small helicopters, which is the reason why the already established rotary wing parameters used in subsection 3.1 are resorted to. The procedure followed here was very similar to that of the previous analysis. Two cases were defined: in the first one the flapping wing shares both the mass and the size (the wingspan of the flapping wing is equal to the rotor's diameter) with the rotary wing vehicle, and in the

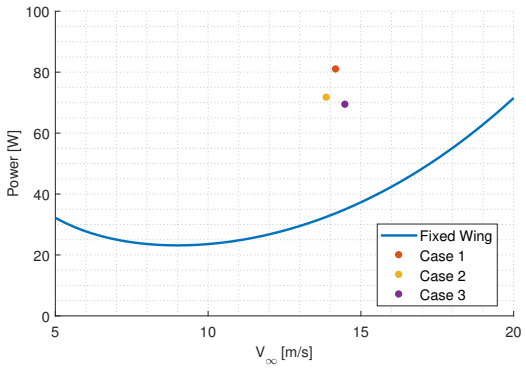

Figure 9: Comparison between different optimized flapping wings and a fixed wing with the same specifications

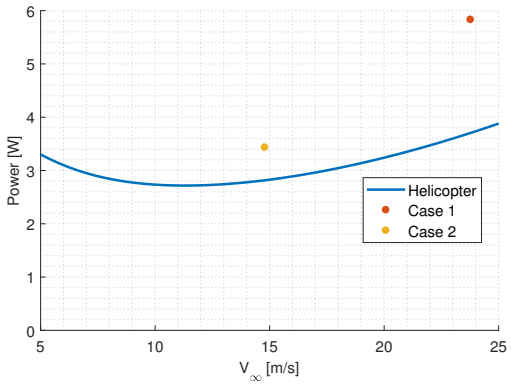

Figure 10: Comparison between different optimized flapping wings and a rotary wing with the same specifications.

second one they only have the same mass. Aside from these factors, every other flapping design variable was free to change at will. Optimizing for the smallest possible power consumption and resorting to the *Steady State Analysis* resulted in the values shown in Table 2.

Parameter	Case 1	Case 2
m [kg]	**0.05**	**0.05**
b [m]	**0.15**	0.26
$\mathcal{AR}$	2.2	2.4
f_{flap} [Hz]	24.1	12.4
V_∞ [m/s]	23.4	14.7
x_f	0	0.16
γ_{max} [°]	77	48
θ_{max} [°]	40	43
θ_{av} [°]	14	13
Lift [N]	0.491	0.491
Thrust [N]	2×10^{-4}	9×10^{-3}
Power [N]	5.76	3.43

Table 2: Parameters and configuration performance metrics resulting from the optimization process.

The comparison of these configurations with the rotary wing is shown in Figure 10. There is not a point where the flapping wing outperforms the rotary wing, but the case 2 shows a power consumption only 22% higher than that of a rotary wing carrying the same payload and moving at the same speed, and the plot also shows how there was a 40% reduction in power consumption by simply being able to use the wingspan as a design parameter. Taking into account that there is room for improvement regarding the wing optimization, the only logical conclusion is that the possibility of designing a flapping wing which is actually preferable in terms of power consumption, compared to a rotary wing, is a very real one.

6. Conclusions

The initial objective of this work was to find out how the flapping wing solution fared against other vehicles, namely the more traditional fixed and rotary wing. In this spirit, the first efforts of the author were directed at trying to find an analytical and *de facto* way to compare different configurations, something quite unusual. The focus then shifted from that, in itself a relatively limited topic, to a much more specific and challenging matter, flapping wing simulation and the implementation of models that could describe such behaviour without resorting to any sort of computationally-heavy method. This opened up several unexpected options like the possibility of modifying and implementing already existing aerodynamic models of hovering flapping wing flight, even creating a whole new model based on the observations made while implementing the simpler ones. From then the natural development was to transform the perfected model into an actual tool, so that it could be used in future studies of flapping wings, and putting it to use by studying how every aspect of the wing design affected its overall success. Then, having found out every parameter's influence on its overall performance, a simple optimization was done, and given that the original objective was to compare these results to those of the typical configurations, this was the final step in this work. In the end this comparison showed that it was possible to obtain a flapping wing that consumed twice as much power as an equivalent fixed wing, and 22% more than a similar helicopter, values that can likely be reduced with an adequate wing optimization process.

Overall, this work produced results in several different fields; firstly, a simple and quick analytical method for comparing different configurations was developed, and the results showed that there were, in fact, situations where each configuration was preferable. On the field of UBET models, two different hovering algorithms were implemented and then successfully modified to suit the forward flight case. To take this a step further, the best parts of each model were taken and fused into a new model, that showed to be very reliable and was therefore used for the last part of this work. The

developed work also led to the creation of a quick, user-friendly tool that can be easily used to study flapping wings, opening up several possibilities in terms of optimization studies and preliminary wing design. Finally, on the topic of the optimization of the flapping wing, the tool was put to the test and a simple optimization was performed. The values that resulted from the optimization could then be collected into several perfected flapping wing designs, and these optimized wings were then compared with the other configurations, finally providing the answer to the question "is a flapping wing really worth it?", which is, in short and in the right circumstances, probably.

6.1. Future Work

The topic of flapping wings is a fascinating one partly because of how unexplored it is. The present work was an attempt at understanding how the aerodynamic mechanisms used by birds and insects work in their favour, to study if those same benefits can be transported to FWMAVs, effectively analysing how viable the implementation of flapping flight to man-made creations is. While some conclusions were drawn in terms of the optimization of flapping wings, this is perhaps the biggest question mark that is left by this work. Can the flapping wing be further optimized and, if so, what is the best procedure to do so?

Furthermore, it would be interesting to put the joint model to the test by seeing how it fares against a CFD simulation, to actually put numbers on the difference that there is between the methods. This would be the definitive test in terms of reliability and accuracy, and, if proven that the difference is not relevant, the present work could actually be considered a viable option to predict the behaviour, the loads and the power consumption of a flapping wing vehicle.

Acknowledgements

The author would like to thank professors Filipe Cunha and João Oliveira for their tireless support and guidance throughout the development of this work.

References

[1] Jung Sun Choi, Jae Woong Kim, Gyung Jin Park, and Do Hyung Lee. Kinematic optimization of a flapping motion for maneuverability and sustainability flights. *Journal of Aircraft*, 50(4):1027–1037, 2013.

[2] Michael H. Dickinson and Sanjay P. Sane. The aerodynamic effects of wing rotation and a revised quasi-steady model of flapping flight. *Journal of Experimental Biology*, 205(8):1087–1096, 2002.

[3] Michael H. Dickinson, Fritz Olaf Lehmann, and Sanjay P. Sane. Wing rotation and the aerodynamic basis of insect flight. *Science*, 284 (5422):1954–1960, 1999.

[4] C. P. Ellington. The aerodynamics of hovering insect flight. ii. morphological parameters. *Philosophical Transactions of the Royal Society of London B: Biological Sciences*, 305(1122): 17–40, 1984.

[5] J. Gordon Leishman. *Principles of Helicopter Aerodynamics*. Cambridge University Press, 2^{nd} edition, 2000.

[6] Zhen Liu and Jean Marc Moschetta. Rotary vs. flapping-wing nano air vehicles: Comparing performances. In *European Micro Air Vehicle Conference and Flight Competition 2009*, pages 114–120, 2009.

[7] Jon N. Ostler, W. Jerry Bowman, Deryl O. Snyder, and Timothy W. McLain. Performance flight testing of small, electric powered unmanned aerial vehicles. *International Journal of Micro Air Vehicles*, 1(3):155–171, 2009.

[8] C. J. Pennycuick. Predicting wingbeat frequency and wavelength of birds. *Journal of Experimental Biology*, 150(1):171–185, 1990.

[9] Umberto Pesavento and Z. Jane Wang. Flapping wing flight can save aerodynamic power compared to steady flight. *Physical Review Letters*, 103 11:118102, 2009.

[10] S.H. Pourtakdoust and S. Karimain Aliabadi. Evaluation of flapping wing propulsion based on a new experimentally validated aeroelastic model. *Scientia Iranica*, 19(3):472 – 482, 2012.

[11] G. Sachs. Comparison of power requirements: Flapping vs. fixed wing vehicles. *Aerospace*, 3 (4):31, 2016.

[12] Q. T. Truong, Q. V. Nguyen, V. T. Truong, H. C. Park, D. Y. Byun, and N. S. Goo. A modified blade element theory for estimation of forces generated by a beetle-mimicking flapping wing system. *Bioinspiration and Biomimetics*, 6(3):036008, 2011.

[13] Jeffrey A. Walker. Rotational lift: something different or more of the same? *The Journal of Experimental Biology*, 205(24):3783–3792, 2002.

[14] L Zheng, T Hedrick, and R Mittal. A comparative study of the hovering efficiency of flapping and revolving wings. *Bioinspiration and Biomimetics*, 8(3):036001, 2013.